State of the Art and Future Trends in the Development of Thermal Barrier Coating Systems

Prakash C. Patnaik
Principal Research Scientist
Structures and Materials Performance Laboratory
Institute for Aerospace Research
National Research Council
Ottawa, Ontario K1A 0R6
CANADA

Xiao Huang
Mechanical and Aerospace Engineering,
Carleton University
Ottawa, Ontario
CANADA

Jogender Singh
Chief Scientist, Applied Research Laboratory
Penn State University
University Park
USA

ABSTRACT

Thermal barrier coating (TBC) systems are the most effective means of protecting structural components from damage caused by excessive temperature and corrosive/erosive environments. The applications for TBCs range from gas turbines and power generators to space and military equipment. As the durability and performance of high temperature components rely more and more on TBCs, the capability of these coatings has become an important variable in the design and development of life prediction models for advanced components that are subject to high temperatures and aggressive environments in service.

In the last decade, the development of TBCs has been driven to a large extent by the demands from the gas turbine industry, with most of the research being focused on improving material chemistry, coating microstructure and processing methods. As a result, a host of new materials, novel microstructures and advanced coating application technologies has been developed which have led to improved thermal insulation capability, durability and stability at higher temperatures, as well as better mechanical properties. These achievements provide new opportunities for designers to redesign existing components and develop new components for gas turbines, as well as space and military systems.

This paper will present the state-of-the-art and future trends in the development of, and applications for, thermal barrier coating systems, with an emphasis on the following three subjects: (1) emerging TBC materials from the zirconate family with increased temperature capability; (2) multiple layered and nano-structured coatings produced by EB-PVD; and (3) new design philosophy and modeling approach for TBC systems with reduced phonon and photon transport.

The current TBC material for gas turbine hot section components is yttria partially stabilized zirconia (YPSZ or YSZ). Zirconia (ZrO_2) has good erosion resistance, a lower intrinsic thermal conductivity and most suitable thermal expansion coefficient as compared to other ceramics such as alumina (Al_2O_3). Yttria (Y_2O_3)

Patnaik, P.C.; Huang, X.; Singh, J. (2006) State of the Art and Future Trends in the Development of Thermal Barrier Coating Systems. In *Innovative Missile Systems* (pp. 38-1 – 38-20). Meeting Proceedings RTO-MP-AVT-135, Paper 38. Neuilly-sur-Seine, France: RTO.

is added into pure zirconia to stabilize the cubic or tetragonal structure and further reduce the thermal conductivity. Recent research has shown that further reduction in thermal conductivity of zirconia based TBCs can be realized by doping or co-doping with transition metal oxides and rare earth oxides. However, the capability of these zirconia based materials is still limited to approximately 1100°C. One of the newest and most promising materials that has the potential to overcome this limitation is zirconate. Zirconate based ceramic material with a pyrochlore structure is stable up to its melting temperature, in the vicinity of 2300°C, and has thermal-insulating properties exceeding those of the more commonly used zirconia based materials. The development of the new zirconate based materials for TBC applications is discussed.

In addition to the chemical composition, the structure of the coating has a significant impact on the thermal and mechanical properties of the coating. Multiple layered or nano-structured coatings, produced by EB-PVD, can reduce heat transport by increasing the number of boundaries between multiple layers or grain boundaries in the coating. Furthermore, the columnar structure produced by EB-PVD is highly strain tolerant, resulting in longer coating life under thermal cycling conditions. A description of the coating process and resulting coating properties is presented.

Finally, a new multiple layered coating structure has been designed by the authors to effectively reflect thermal radiation. The coating system consists of sets of highly reflective multiple layers of ceramic stacks and a single layer of ceramic material with low thermal conductivity and low refractive index. Specifically, within the multiple layered stacks, each is designed to reflect a targeted range of wavelength, utilizing alternating layers of ceramic materials with low and high refractive indices. In this manner, when a suitable number of stacks are selected according to the application temperature, a broadband reflection of the required wavelengths can be achieved. A computational method has been developed to predict the temperature distribution within the multiple layered TBC system. At an assumed service environment temperature of 1727°C, a temperature reduction of as much as 90°C can be realized on the metal surface when a 250μm multiple layered coating is used instead of a monolayered coating of the same thickness. The design philosophy and the development of computational methods are presented.

1.0 INTRODUCTION

Thermal barrier coating (TBC) systems are the most effective means to protect structural components from damage caused by excessive temperature and corrosive/erosive environments. The applications for TBCs range from gas turbines and power generators to space and military equipment. As the durability and performance of high temperature components rely more and more on TBCs, the capability of these coatings has become an important variable in the design and development of life prediction models for advanced components that are subject to aggressive environments.

A typical TBC system is shown in Figure 1. The top ceramic layer is directly exposed to the hot environment and functions as a thermal barrier by retarding the heat flow from the hot environment to the metal substrate. The basic requirements for the top layer material are: (1) good thermal insulation, i.e., low thermal conductivity and low transparency to thermal radiation; (2) high melting and phase stability at operating temperatures; (3) high thermal expansion coefficient to reduce thermal stress; (4) erosion resistant in order to prevent impact damage caused by ingested particles such as sand and silicates during operation; (5) oxidation or hot corrosion resistant; and (6) thermodynamic compatibility with bond coat and thermally grown oxide (TGO) [[1]]. The currently preferred material used for gas turbine hot section components is yttria partially stabilized zirconia (YPSZ). Placed between the ceramic layer and the superalloy substrate is a MCrAlY (M = Ni, Co or NiCo) metallic bond coat. The bond coat is used for protecting the substrate from oxidation

and high temperature corrosion, as well as providing for improved adhesion of the ceramic to the metal substrate via the formation of a thin, uniform and defect free α-Al_2O_3 layer at the ceramic/bond coat interface. This thin α-Al_2O_3 layer is conventionally called thermally grown oxide (TGO), which has very low oxygen ionic diffusivity and thus provides an excellent diffusion barrier to oxygen transport at high temperatures [[2]].

In the last decade, the development of TBCs has been driven primarily by the demands of the gas turbine industry, with most research focusing on reducing thermal conduction through the ceramic coatings by improving material chemistry, coating microstructure and processing methods. Pure zirconia experiences a phase transformation from tetragonal to monoclinic during cooling. This results in a change in volume and can lead to cracking. For this reason, metal oxides such as CaO, MgO, CeO_2, Sc_2O_3, Y_2O_3 and other rare earth metal oxides are added into ZrO_2 to stabilize both cubic and tetragonal structure of zirconia to room temperature. For dopants with valence less than +4, oxygen vacancies are generated within the ionic lattice to maintain electrical neutrality. These vacancies strongly scatter phonons by virtue of both missing mass and missing interatomic linkage and therefore result in a decrease in thermal conductivity [[3]]. Of these metal oxides, Y_2O_3 – stabilized ZrO_2 (YSZ) is found to be the most suitable dopant for TBC applications [[4], [5], [6]]. The optimum amount of yttria to add to zirconia has been found to be around 7~8 wt % (4~4.5 mol %). This composition offers the highest degree of resistance to spallation and excellent thermal stability [[5], [7],[8]].

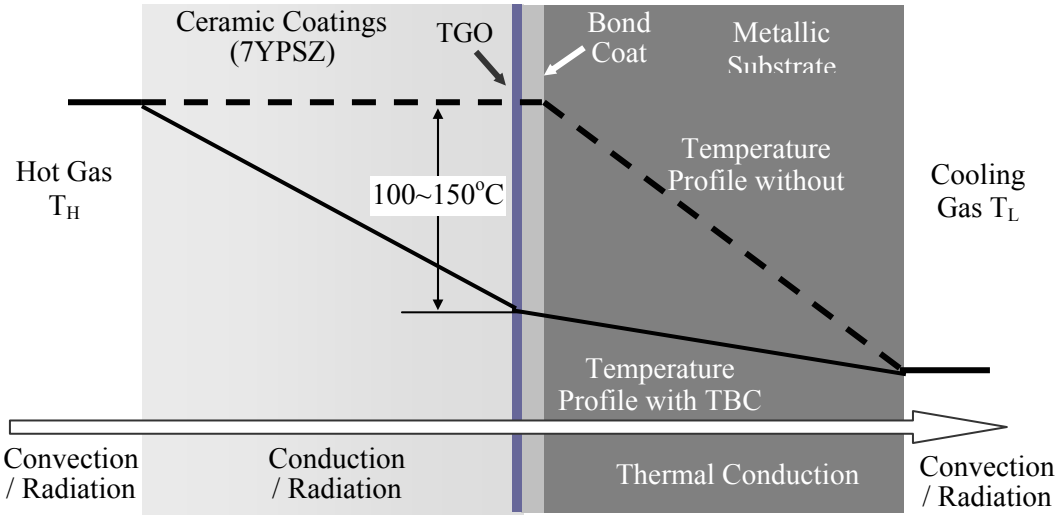

Figure 1: Schematic of TBC system in a gas turbine environment.

Further reduction in the thermal conductivity of YSZ through yttria addition is limited by the need to stabilize the tetragonal *t'*- phase structure [[8]]. In order to incorporate more scattering centers without affecting the crystal structure, transition metal oxides and rare earth oxides have been doped or co-doped into YSZ. For example, the thermal conductivities of 4 mol % Y_2O_3 + ZrO_2 system doped with an additional 4 mol % of Yb_2O_3, Er_2O_3, Gd_2O_3 or Nd_2O_3 have been studied and shown to reduce the thermal conductivity in general. However, Fadolinia was found to be the most effective dopant [[9]]. A multi-component defect-clustering approach has also been shown to be very effective. In this approach, a group of selected oxides including ZrO_2- Y_2O_3 - Nd_2O_3 (Gd_2O_3, Sm_2O_3) - Yb_2O_3 (Sc_2O_3) is co-doped into conventional zirconia- and hafnia-yttria

oxides [[10]]. These oxides create thermodynamically stable, highly defective lattice structures with essentially immobile defect clusters and/or nanoscale ordered phases. With this defect clustered structure, a significant reduction in thermal conductivity is achieved and sintering resistance is also improved. For the $ZrO_2 – M_2O_3$ binary system, a semi-empirical phonon model indicated that there is a linear trend of decreasing thermal conductivity with increasing cation size of the dopant for partially stabilized YPSZ, DyPSZ and SmPSZ [[11], [12]].

The performance of TBCs depends not only on the intrinsic properties of the TBC materials, but also on the coating's microstructure. The most widely used industrial deposition processes for the application of TBCs are Plasma-Spraying (PS) and Electron Beam Physical-Vapor-Deposition (EB-PVD). The TBCs produced by PS process have a laminar structure, consisting of splats with inter-splat pores and cracks parallel to the coating surface, as shown in Figure 2a. TBCs produced by EB-PVD, on the other hand, have a columnar microstructure (Figure 2b) with elongated grains and pores aligned perpendicular to the coating surface, enabling very high levels of stress compliance [[13]].

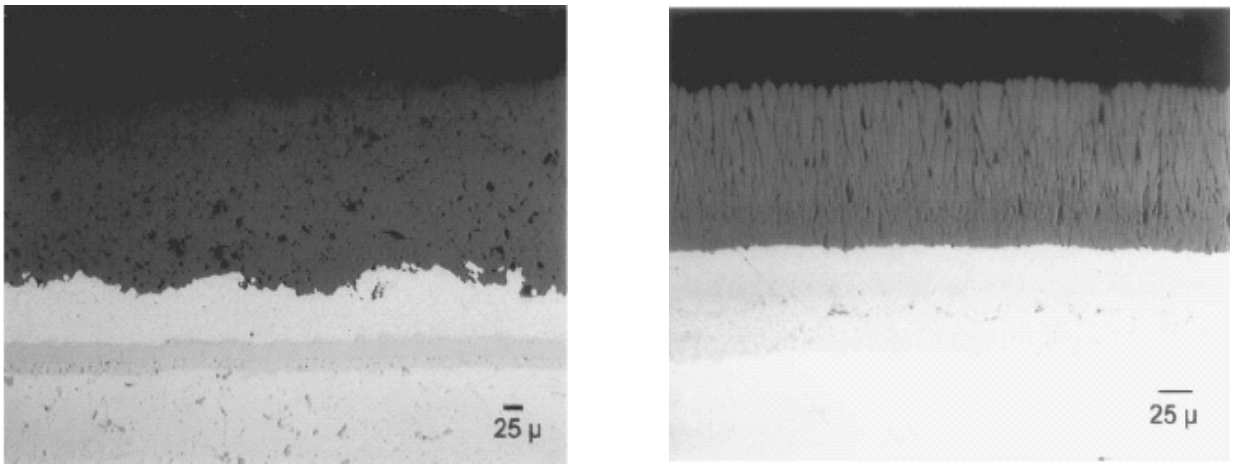

(a) (b)

Figure 2: Photomicrographs of (a) an APS applied TBC showing a laminar structure and (b) an EB-PVD applied TBC showing a columnar structure [[13]].

One of the disadvantages of EB-PVD applied coatings is a higher thermal conductivity than that of APS applied coatings. The coatings produced by PS typically have a thermal conductivity of 0.9~1.1W/mK at room temperature due to the micro-cracks and the high volume fraction of inter-splat pores that are predominantly aligned parallel to the coating surface. The coatings applied using EB-PVD have a thermal conductivity in the range of 1.3~2.0W/mK [[22]].

The microstructure and pore morphologies in thermal barrier coatings have a significant effect on the thermal conductivity. In order to couple the pore morphology that offers the highest impedance to heat flow with the columnar microstructure thereby optimizing thermal and mechanical performance, a novel thermal barrier coating that exhibits a columnar structure with zig-zag morphology pores was developed using electron beam-directed vapor deposition (EB-DVD) technology [[14]]. This EB-DVD deposited zig-zag TBC with a 13.1 µm wavelength achieved a thermal conductivity value of 0.8W/mK at room temperature [[15]]. Another modification which may be made to the columnar structure is the introduction of layered interfaces into the

EB-PVD coating without disrupting the columnar structure [[9], [16]]. In this method, the layers in each column are parallel to the coating surface, and the densities are changed from layer to layer by switching the D.C. bias applied to the substrate between high and low levels during deposition. The measured thermal conductivity of this microstructure showed a 45% reduction.

It is well known that increasing operating temperatures will improve the performance of gas turbine and diesel engines. However, further increases in operating temperatures bring out two considerable issues, namely decomposition of tetragonal t' phase of 7YSZ at increased operating temperatures and increased thermal radiation.

At temperatures above 1200^{o}C, the yttria partially stabilized zirconia based coatings exhibit destabilization of the tetragonal t' phase to yttria-poor tetragonal and yttria-rich cubic. On cooling from service temperature, the tetragonal phase will transform into monoclinic phase and result in cracking in the coating [[8], [17], [18]]. Additionally, at temperatures higher than 1100^{o}C, sintering of Y-PSZ will occur which results in an increase in Young's modulus and thermal conductivity, and thus shortens the life of the coating [[19], [20]]. Furthermore, yttria partially stabilized zirconia is oxygen transparent at high temperatures and when combined with porosity and cracks inside the coatings, it causes the bond coat of TBC system to be more susceptible to oxidation attack, with increased formation rate of undesirable oxides such as NiO and $Ni(Cr, Al)_2O_4$ near the bond coat [[20]].

The intrinsic thermal conductivity of ceramic coatings has an inverse dependence on the temperature according to thermal conductivity theory. However, the measured thermal conductivities are found to increase with temperature for both zirconia- and zirconate- based ceramic coatings [[22], [23], [24]]. This increase in thermal conductivities at high temperatures is attributed to thermal radiation since the TBC materials are partially or fully transparent to thermal radiation at typical engine operating temperatures. The optical properties of yttria-stabilized zirconia within the wavelength range of 0.3 ~ 10μm is given in Figure 3 [[25]]. As seen in this figure, the thermal radiation can transmit directly through zirconia based TBC coatings to the metal substrate. At typical operating temperatures, more than 90% of the radiation falls within the transparent region of YPSZ [[9]] and as much as 50^{o}C of temperature increase on metal substrate can result [[26]]. Thus, to increase the thermal insulation capability of TBCs, both thermal conduction and thermal radiation must be considered.

The following three sections summarize recent developments in TBCs in three directions: (1) emerging TBC materials from the zirconate family with increased temperature capability; (2) multiple layered and nano-structured coatings produced by EB-PVD; (3) new design philosophy and modeling approach for TBC systems with reduced phonon and photon transport.

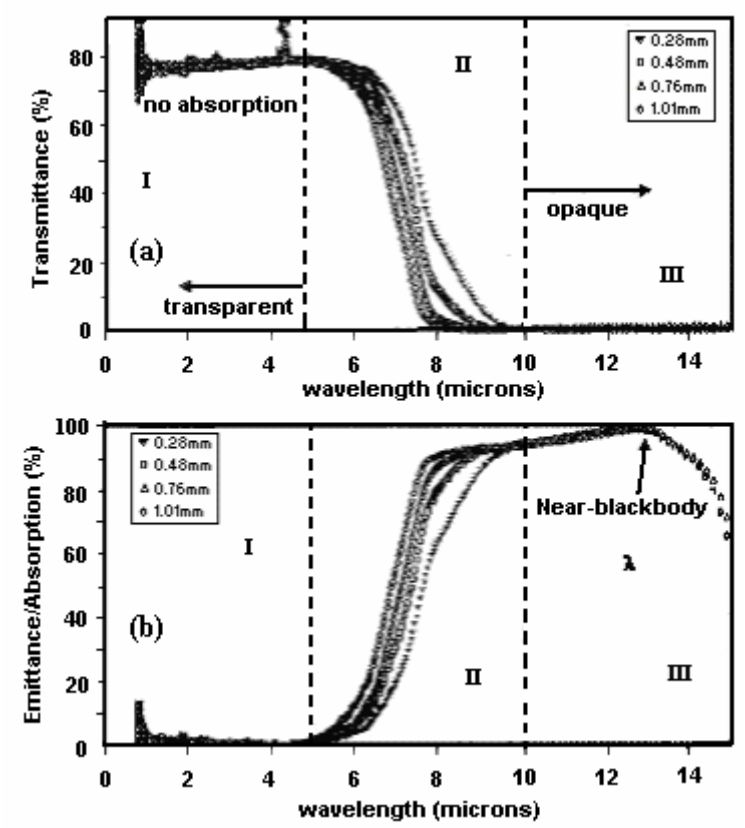

Figure 3: Room temperature (a) hemispherical transmittance; (b) hemispherical emittance / absorptance along (100) direction of single crystal 13.5 YSZ specimens with various thickness [[25]].

2.0 EMERGING TBC MATERIALS WITH INCREASED TEMPERATURE CAPABILITY

The rare-earth zirconates, such as $La_2Zr_2O_7$, $Nd_2Zr_2O_7$ and $Ga_2Zr_2O_7$ are among the most promising TBC materials for the future. The zirconates have a typical composition of $A_2B_2O_7$ and a cubic pyrochlore structure [[27], [28]], as shown in Figure 4. The pyrochlore phase is stable up to its melting point at 2300^0C [[29]], making them potential TBC materials for higher application temperatures.

One of the basic requirements for potential TBC materials is a low intrinsic thermal conductivity, which has been found to be associated with the complexity of crystallographic structure and difference in the number and types of atoms in a unit cell [[30], [31]]. The pyrochlore structure is similar to the fluorite structure assumed by YSZ but with one missing oxygen atom, and a large number of displaced oxygen atoms. As such, the pyrochlore crystal can be considered as an ordered, highly defective fluorite solid solution with reduced symmetry and more complicated structure, thereby exhibiting reduced intrinsic thermal conductivity. It has been experimentally confirmed that the thermal conductivities of rare earth zirconates are much lower than that of 7YSZ [[29], [32], [37]]. At 1000^oC, the thermal conductivities are 1.5~1.6 W/m·K and 1.2~1.3 W/m·K for dense $La_2Zr_2O_7$ and $Nd_2Zr_2O_7$ respectively [[29]]. At 700^oC, the thermal conductivity values range from 1.5 to 1.6 W/m·K for dense $Gd_2Zr_2O_7$, $Nd_2Zr_2O_7$ and $Sm_2Zr_2O_7$ while the thermal conductivity of dense 7YSZ is 2.3 W/ m·K [[32]].

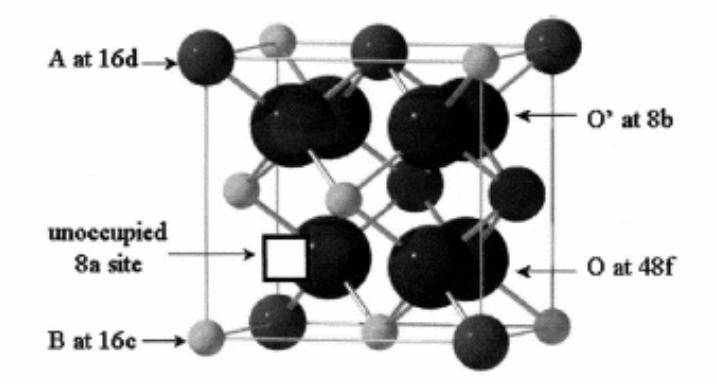

Figure 4: Schematic of the partial unit cell of the pyrochlore structure [[28]].

Among these zirconates with low thermal conductivities, lanthanum and zirconium have similar vapor pressure which makes vapor deposition more readily possible [[33]]. Additionally, an atomistic simulation indicated that the rare earth zirconates have higher oxygen anion Frenkel pair energy than yttrium and therefore it requires higher activation energy for oxygen migration [[27], [34], [35]]. This characteristic of reduced oxygen transparency of lanthanum zirconate provides better bond coat oxidation resistance than YSZ can offer [[36]].

However, the low thermal expansion coefficients of the rare earth zirconates may lead to higher thermal stresses during thermal cycling as compared to 7YSZ, although the Young's moduli of the zirconates are about 15% lower and to some extent could compensate for the effect of the higher mismatch in thermal expansion coefficient and alleviate the stress. The values of thermal expansion coefficients as well as Young's moduli for selected zirconates are given in Table 1.

Table 1: Thermal expansion coefficients and Young's modulus of zirconates.

Material	Thermal expansion coefficient ($x10^{-6}$ K^{-1})	Young's modulus (Gpa)
$Gd_2Zr_2O_7$	8.1~10.5 at 200~1000°C [[29]]	
$Eu_2Zr_2O_7$	10.3~10.6 at 200~1000°C [[29]]	*205 [[35]]
$Nd_2Zr_2O_7$	9.0~9.7 at 200~1000°C [[29]]	*219 [[35]]
$La_2Zr_2O_7$	8.1~9.1 at 200~1000°C [[29]]	175±1 [[37]]
$Sm_2Zr_2O_7$	10.8 [[34]]	*231 [[35]]
7YSZ	11.5 at 200~1000°C [[38]]	*250 [[32]] / 210±10 [[37]]

Further research also indicates that the pyrochlore zirconates readily form β-alumina or perovskite between the TBC and TGO by diffusion and are therefore not thermodynamically compatible with TGO [[39]].

Further research is required to fully explore the potential of these zirconate based ceramic materials and to identify a more suitable bond coat if zirconates are to be used on superalloy substrates.

3.0 MULTIPLE LAYERED AND NANO-STRUCTURED COATINGS PRODUCED BY EB-PVD

Typical microstructures of TBC produced by EB-PVD can be divided into two zones: an inner zone and an outer zone. The inner zone is the early part of multiple nucleation and subsequent growth of the columnar microstructure having large number of interfaces, grain boundaries, microporosity and randomly oriented grains. The inner zone ranges from 1 to 10μm in thickness and exhibits lower thermal conductivity (~1.0 W/m. K). The outer part of the coating is crystallographically more perfect, with fewer grain boundaries. The thermal conductivity in this zone approaches that of bulk zirconia (2.2 W/m. K). Therefore, the apparent thermal conductivity of the EB-PVD coating will be higher than that of the inner part of the coating. The thicker the outer part is, the higher the thermal conductivity. If the coating deposited by EB-PVD consists of multiple layers with microstructure similar to that of the inner zone of regular EB-PVD coating without sacrificing other desirable properties, then the apparent thermal conductivity can be reduced significantly. This modified coating has been developed by creating periodic strain fields within the TBC during the EB-PVD deposition process. It consists of multiple layers, each layer having a microstructure similar to that of the inner zone of the initial EB-PVD coating, as shown in Figure 5. The increased phonon scattering centers caused by a number of interfaces, grain boundaries, as well as microporosity within each layer, therefore result in a reduction in thermal conductivity. Figure 6 shows the measured thermal conductivity of the EB-PVD coating as a function of the total number of layers produced by the "shutter" method. There is a 30% reduction in thermal conductivity for the 20 layers of coating [[16]].

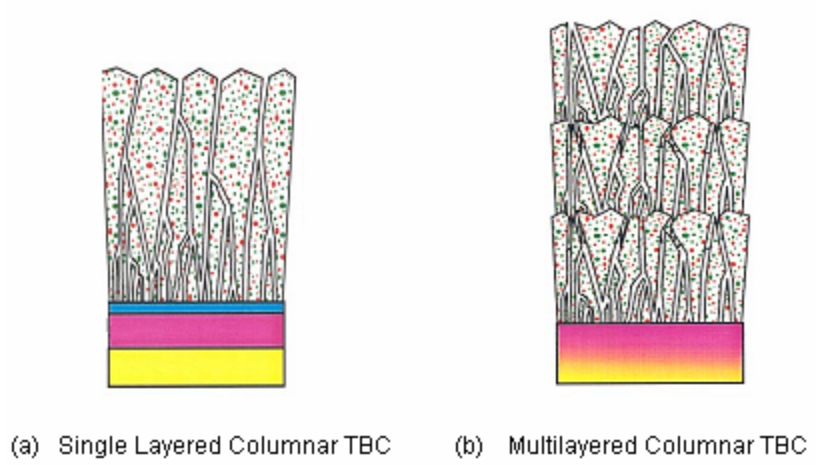

Figure 5: Typical standard vapor phase columnar structure and modified columnar microstructure with multiple interfaces.

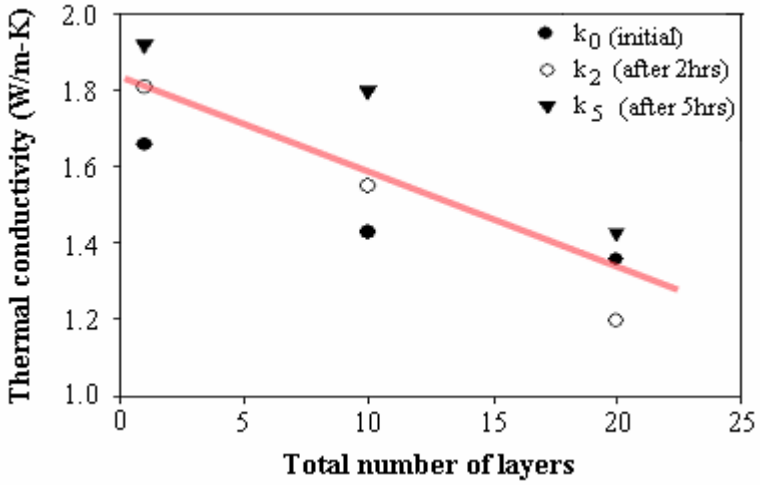

Figure 6: Thermal conductivity of EB-PVD as a function of total number of layers produced by the "shutter" method, measure at various stages of testing, where k_0 = as deposited, k_2 = after 2hrs, and k_5 = after 5hrs of testing.

In addition to reducing the thermal conductivity, modifying the microstructure also decreases the thermal radiation transport through the TBC by increasing the hemispherical reflectance of the coating as well. A high hemispherical reflectance is produced as a result of the difference in the refractive indices of the alternate layers within a multiple layer structure, achieved by periodically interrupting incoming vapor flux during depositing process to vary the densities of alternate layers since the variation of densities results in different refractive indices. The use of two or more ceramic materials with different chemical compositions, such as 8YSZ with high refractive index and Al_2O_3 with low refractive index, is another route to produce multiple layered coating with high reflectance. A multiple layered structure with alternating 400 nm 8YSZ and 100 nm Al_2O_3 is shown in Figure 7. The hemispherical reflectance was increased from 35% (single layer) to 45% (20 layers) to radiation at 1μm wavelength, as shown in Figure 8. However, to effectively reflect a broadband radiation, an optimized design is required for such multiple layered coatings.

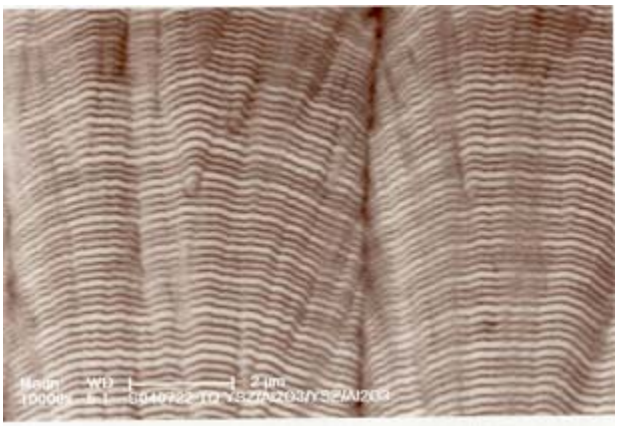

Figure 7: Multiple layered 8YSZ/Al_2O_3 structure with increased hemispherical reflectance.

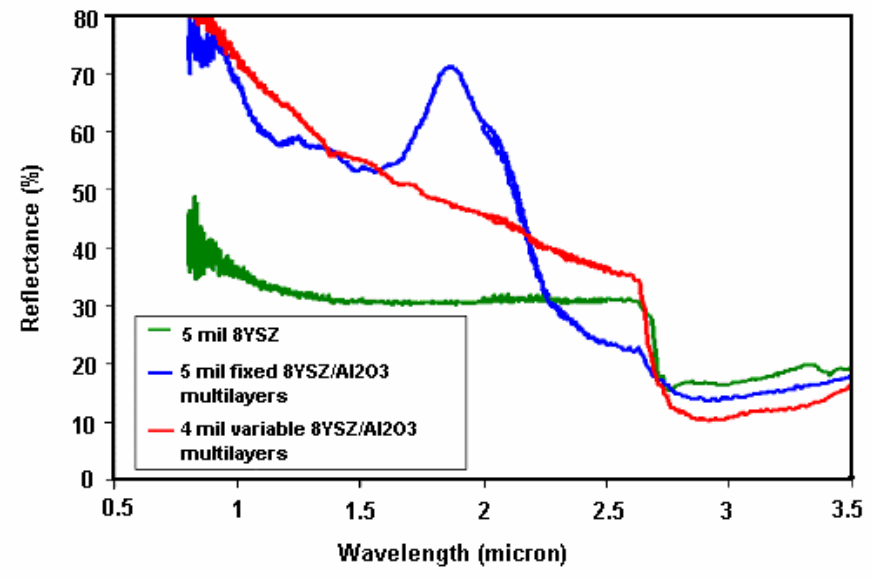

Figure 8: Multilayered TBC increases IR reflectance with fixed and variable spacing.

4.0 NEW DESIGN PHILOSOPHY AND MODELING APPROACH FOR TBC SYSTEMS WITH REDUCED PHOTON AND PHONON TRANSPORT

In this section, a new multiple layered high reflective coating system designed by the authors will be presented. The multiple layered TBC system consists of a set of high reflectance multiple layered ceramic stacks (M) that are designed to reflect thermal radiation, in the wavelength in the range of 0.45~5μm, a single ceramic layer (S) with low thermal conductivity, a bond coat and the metal substrate. This wavelength range is based on the typical operating temperature of 1700~2000K in a gas turbine combustion environment.

Within the multiple stacks M, each stack is designed to reflect a targeted range of wavelength. A broadband reflection for the required wavelength range can be obtained using sufficient number of stacks. To achieve high reflectance for each wavelength range, each stack must have multiple layers of ceramic materials with alternating high and low refractive indices and the optical thickness of each layer must be equal to a quarter-wavelength in order to meet the condition of multiple-beam interference. Considering that the radiation with shorter wavelength will be scattered much more strongly within the coatings, the stack reflecting shortest wavelength range is therefore arranged on top of the multiple layer stacks, and the stack reflecting the longest wavelength range is at the bottom of the multiple layered stacks. Since scattering in thin film coating is caused mainly by the interface roughness and pores within the coatings, the coating process and coating materials will be investigated to obtain an ideal structure in order to have high reflectance and lower thermal conductivity. Figure 9 shows schematically how the radiation is reflected or transmitted through these multiple layered stacks.

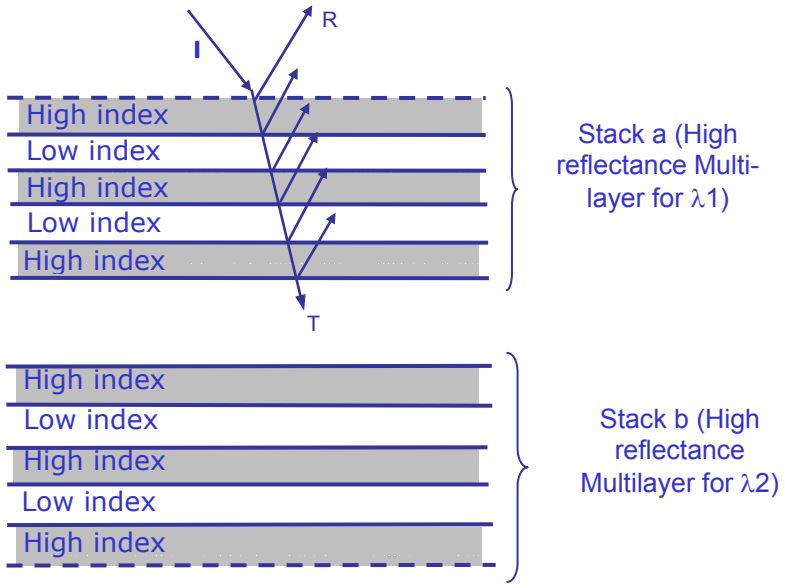

Figure 9: Schematic diagram of high reflectance multiple layered TBC structure.

The function of single ceramic layer (S) is to reduce the phonon transport through the TBC system. It is therefore desirable to select a material with low thermal conductivity for this single layer. There are two configurations for the S layer design. If the single layer is designed to be placed on the top of multiple layered stacks, the material for the single layer is also required to have low scattering coefficient and low refractive index. This low refractive index ensures decreased internal reflection at the interface I and minimum internal radiation emission in this layer [[40]]. The selection of low scattering coefficient is to make certain that the reflected radiation from high reflectance multiple layers will not be scattered back. In addition, the single ceramic layer, when placed on the top, is directly exposed to the hot environment, and therefore phase stability is very critical for the performance of the TBC system. A zirconate based ceramic material with pyrochlore structure is potentially the best choice for the top single layer. On the other hand, if the single ceramic layer is placed between the multiple layered stacks and the bond coat, zirconates may not be suitable materials since they are not thermodynamically compatible with Al_2O_3 near the bond coat. The doped 7YSZ may provide another option. However, the selection of materials and the related physical and optical properties have to be optimized systematically based on the temperature distribution through the designed system.

The multiple layered stacks can be designed by calculating the physical thickness of each layer in one stack using [[41]]:

$$d_H(\lambda) = \lambda/(4n_H) \qquad \text{(Eq. 1)}$$

$$d_L(\lambda) = \lambda/(4n_L) \qquad \text{(Eq. 2)}$$

where d_H and d_L are thicknesses for the alternating layers within the stack, and n_H and n_L are the refractive indices of the alternating layers. H denotes layer with high reflective index and L denotes layer with low reflective index. λ is the radiation wavelength.

Assuming that the absorption and scattering of the radiation in the high reflectance stacks are negligible, the reflectance for one wavelength range is then given by:

$$R = \left(\frac{\eta_0 B - C}{\eta_0 B + C}\right)\left(\frac{\eta_0 B - C}{\eta_0 B + C}\right) \quad \text{(Eq. 3)}$$

where

$$\begin{bmatrix} B \\ C \end{bmatrix} = \left(\prod_{r=1}^{q} \begin{bmatrix} \cos\delta_r & (i\sin\delta_r)/\eta_r \\ i\eta_r \sin\delta_r & \cos\delta_r \end{bmatrix} \right) \begin{bmatrix} 1 \\ \eta_m \end{bmatrix} \quad \text{(Eq. 4)}$$

and

$$\delta_r = 2\pi n_r d_r \cos\theta_r / \lambda \quad \text{(Eq. 5)}$$

and η_0, η_r and η_m are the optical admittances for incident medium, multiple layers M and substrate, respectively. θ_r is the incident angle, d_r is the layer thickness, n_r is the refractive index of each layer, r is the layer number and q is the total number of layers within a stack.

For p-wave, $\eta_p = \dfrac{2.6544\times10^{-3} n}{\cos\theta}$; and for s-wave, $\eta_s = 2.6544\times10^{-3} n\cos\theta$.

Under normal incidence condition, the reflectance in air or free space for one wavelength range is expressed as:

$$R \approx 1 - 4\left(\frac{n_L}{n_H}\right)^{2p} \frac{n_m}{n_H^2} \quad \text{(Eq. 6)}$$

The width of the high-reflectance wavelength zone is:

$$\Delta\lambda = \frac{2\lambda}{\pi} \sin^{-1}\left(\frac{n_H - n_L}{n_H + n_L}\right) \quad \text{(Eq. 7)}$$

where n_m is the refractive index of substrate.

Assuming n_L =1.5, n_m = 2.2, and n_H = 2.2, the number of stacks and layers as well as the physical thickness of each layer can be calculated. Under an isotropic hemispherical incidence condition, multiple layered stacks consisting of 10 stacks and a total of 79 layers produce a hemispherical spectral reflectance as given in Figure 10. The wave length range for this calculation is 0.45~5 μm and detailed method is given in Ref. [[41]].

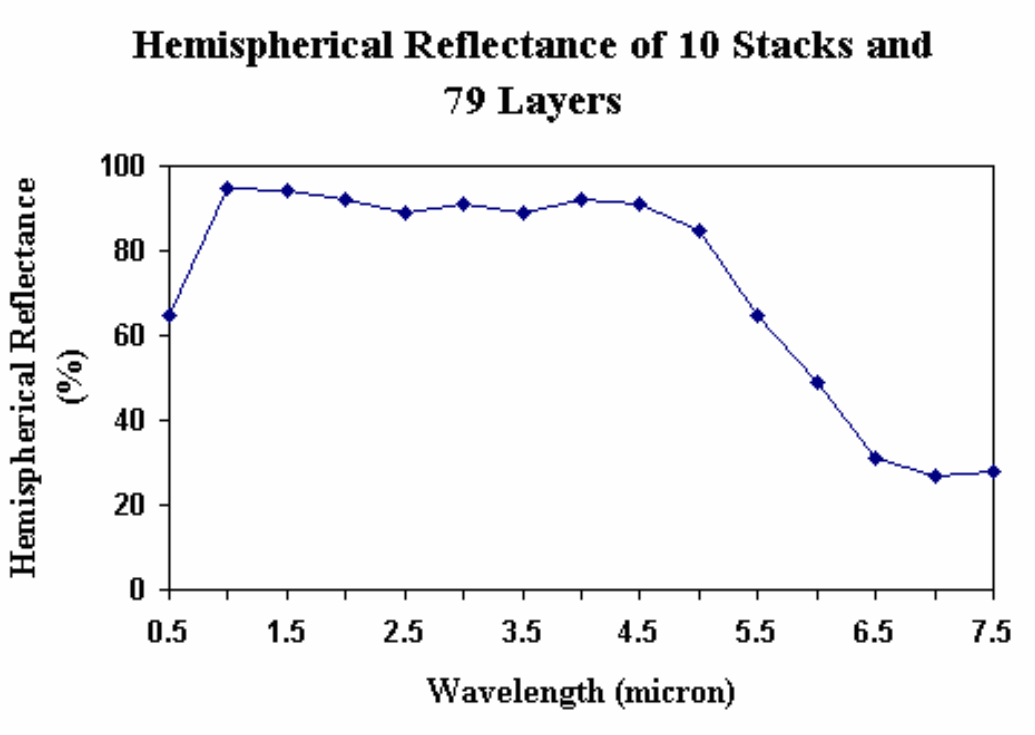

Figure 10: Calculated hemispherical reflectance of 10 stacks with 79 layers.

Consider a multiple layered thermal barrier coating system in an environment typical of a gas turbine engine. The ceramic coating surface is exposed to the hot gases and heated by convection that results in a temperature increase on the coating surfaces. Assume that the heat transfer has reached a steady state, and there is no other heat source inside the system. Thus, the total heat flux reaches a constant. Within the single ceramic layer and multiple layered stacks, the heat is transferred by thermal conduction and thermal radiation.

For a one dimensional heat transfer condition, the energy equation can be expressed as:

$$Q_{tot} = -k_j \frac{dT_j(x_j)}{dx_j} + q_{rj}(x_j) \qquad j = \begin{cases} S \\ 1,2,...n \end{cases} \qquad \text{(Eq. 8)}$$

where S is the subscript index for single ceramic layer, n is the number of coating layers. Q_{tot} is the total heat flux within the coatings, $q_{rj}(x_j)$ is the radiation flux at x position of the jth layer of the coatings along x direction, k_j is thermal conductivities of the jth layer and $T_j(x_j)$ is the temperature at x position of the jth layer of the coatings.

Within the metal substrate, all the radiation flux has been absorbed and converted into heat due to the opaque characteristic of metallic materials and there is only thermal conduction mode of heat transfer. Thus we have

$$Q_{tot} = -k_m \frac{dT_m(x_m)}{dx_m} \qquad \text{(Eq. 9)}$$

where k_m is thermal conductivity of metal substrate and $T_m(x_m)$ is the temperature at x_m position within the metal substrate. Here the bond coat is assumed to be thin enough that the temperature difference between the bond coat and metal substrate is neglected. Detailed procedures used to solve the above energy equations were reported in reference [[42]].

Consider the two structures, as illustrated in Figure 11 (A) and (B). In structure (A), the single layer is placed on top of the multiple stacks while in structure (B), the single layer is placed under the bottom of multiple stacks. In the computational analysis presented here, both Al_2O_3 (with refractive index n_L = 1.5 and thermal conductivity k_L = 2.4 $Wm^{-1}K^{-1}$) and 7YSZ (with refractive index n_H = 2.1 and thermal conductivity k_H = 0.8 $Wm^{-1}K^{-1}$) were selected as the material for alternating layers in the multiple stacks. Other properties such as the refractive indices and the spectrum properties are based on published values in references [[25]] and [[26]]. The temperature distributions within the coatings and the total heat flux through the TBC system for these two coating structures are calculated by solving radiation transfer equations and heat transfer equations using methods detailed in reference [[42]]. The total thickness of the multiple layered coating is assumed to be 250 μm whereas the thickness of the high reflectance multiple layered stacks is 50 μm. For comparison purposes, a mono-layered coating of the same total thickness was used as the base line in the computational analysis. The calculated temperature distributions are shown in Figure 12.

It is found from the results that structure B can achieve the most significant temperature reduction on the metal substrate. At an assumed environment temperature of 1727^0C (2000 K), temperature reduction of 90^0C can be achieved when structure B is used instead of a mono-layered coating of the same thickness. When structure A, where multiple layered stacks placed on top of the single layer is used, a temperature reduction of 46^0C can be realized on the metal surface when compared to that of mono-layered coating of the same thickness. It is clear that the high reflectance multiple layered coating systems, irrespective of the layer arrangement, can effectively reduce the temperature on the metal surface by reducing the radiation entering into the coating system.

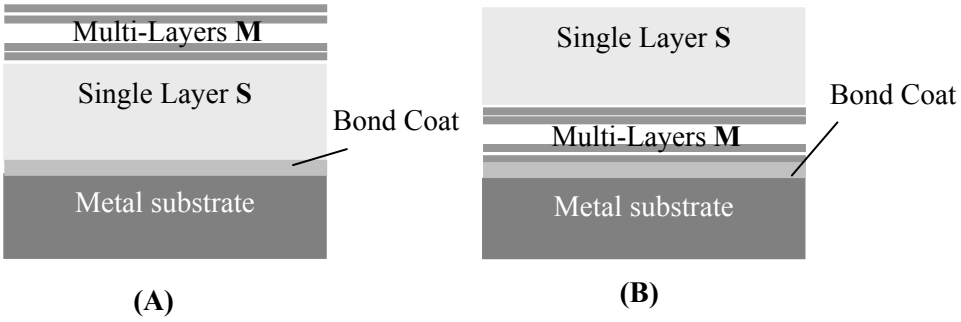

Figure 11: Schematic of new designed multiple layered high reflectance TBC structures.

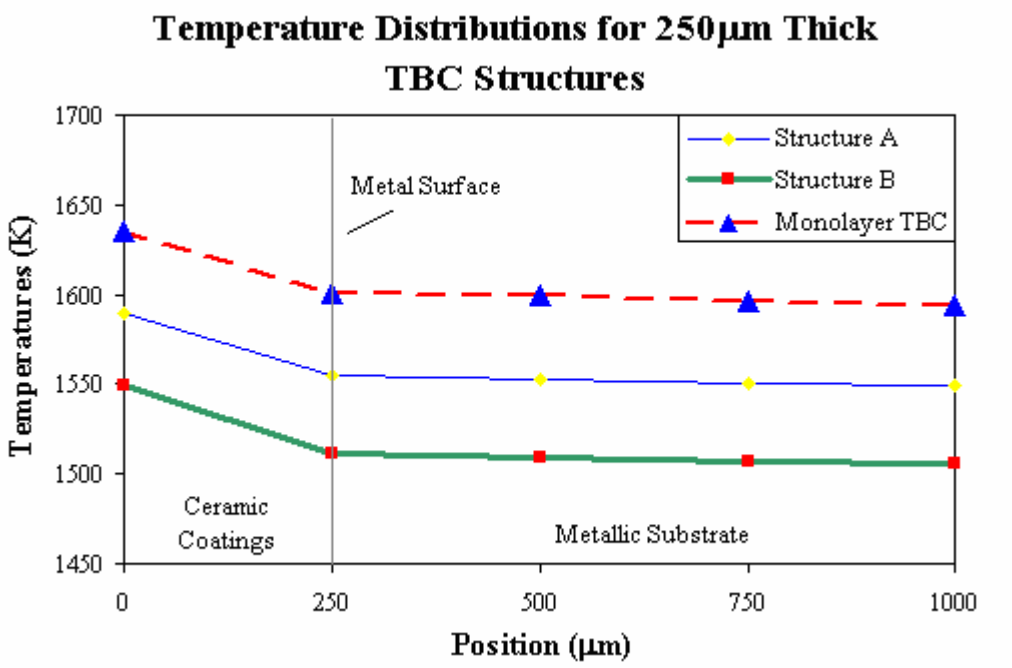

Figure 12: Computed temperature distributions for 250μm thick multiple layered coating compared with mono-layered coating. Design structure A: multiple layers on the top of the single layer; Design structure B: single layer on the top of multiple layers.

Comparing the temperatures given in Figure 12, it is found that in addition to the observed temperature decreases on the metal surface, the temperature on the coating surface can also be significantly reduced when structures A and B are used. In contrast to the temperature on the coating surface of mono-layered coating structure, structures A and B achieved further surface temperature reductions of 46°C and 86°C, respectively. This is attributed again to the effective reduction of radiation entering the coating system. This reduction in coating surface temperature could play a significant role in extending coating's useful life.

Further analysis is carried out to compute the temperature distributions within the coatings and metal substrate for both structures A and B with increasing total coating thickness from 250μm to 1000μm. In this simulation, the thickness for multiple layered stacks (S) is kept at a constant value of 50 μm. The temperature reduction on the metal surface is obtained using the difference in temperature resulting from using multiple layered coating and mono-layered coating of the same thickness. It can be seen from Figure 13 that the reductions in temperature on the metal surface for both structures are less pronounced when the total coating thickness is further increased. Coating structure B, where the single layer is placed on the top of multiple layered stacks, again offers better protection to the metal substrate than structure A of the same thickness.

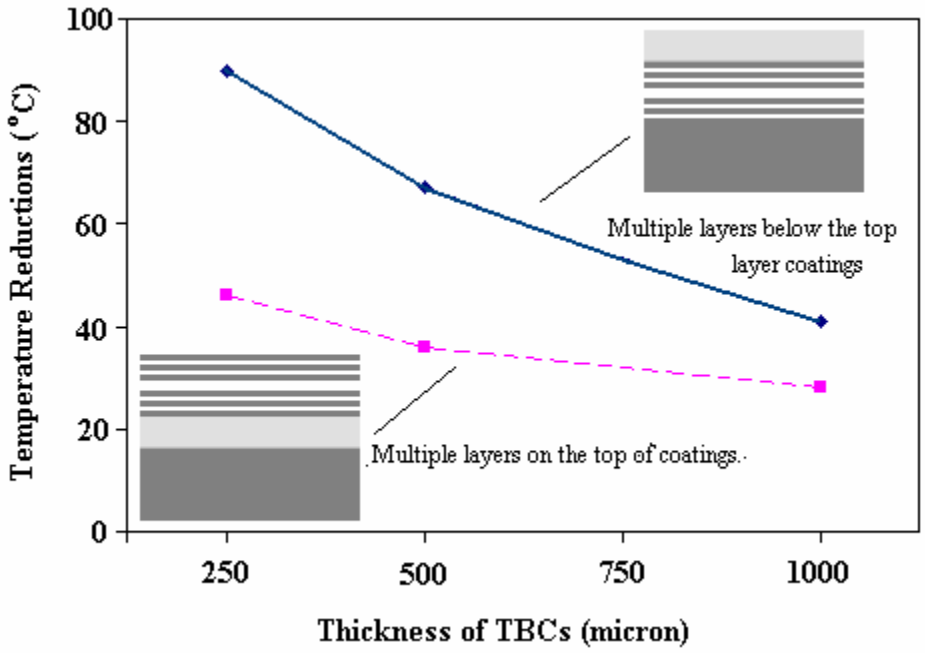

Figure 13: Computed temperature distributions for multiple layered coatings with varying total thickness. The multiple layered stacks are kept to be 250μm and mono-layered coating of the same thickness is used as the base line.

In the simulation described, the effect of grain and layer boundaries on thermal conductivity was not considered. However, from the theory of grain boundary phonon transport, the phonon mean free path is governed by the layer thickness. The thinner the coating layer thickness, the shorter the phonon mean free path. As such, the effective thermal conductivity of the high reflectance multiply layered stacks may be further reduced due to the nano-dimensional grains or layers. It is anticipated that the high-reflectance multiple layered coating system can reduce both photon and phonon transport through the TBC system. Further analysis using a finite element approach is being conducted at present to include this thermal conductivity reduction as a result of the nano-scaled multiple layered structure.

Multiple layered coating structures, with periodically repeated structure throughout the coatings, have been examined by several researchers [[9], [16]] and reduced thermal conductivity associated with multiple layering has been reported. While the metal substrate can be further protected when these coats are applied, the high temperature stability of these multiple layered coatings presents challenges and limitation to their practical use in gas turbine engines. If multiple layers are present on the surface of the coating structure, they will inevitably experience the highest temperature of the environment and are subject to coating failure such as by spalling, interdiffusion and other phase transformation and sintering related damages. It is therefore crucial to ensure that the multiple layers used to reflect radiation are shielded from the most severe environment such as that in structure B. However, this shielding/top layer should be selected to ensure a low scattering nature. Otherwise, as shown in this study, the multiple layered structures will not function in the most optimum condition.

5.0 CONCLUSION

The latest developments in thermal barrier coatings is summarized in this paper with focus on the three most promising research directions, namely emerging TBC materials from the zirconate family, multiple layered and nano-structured coatings produced by EB-PVD and new design philosophy and modeling approach for TBC systems with reduced phonon and photon transport. While these new materials and structures have not yet found commercial applications, it is certain that the current TBCs based on 7YSZ will no longer meet the demand for future gas turbine applications. New materials and processing technologies will be required and emerge in the near future.

6.0 REFERENCES

[1] D. R. Clarke and C. G. Levi, "Materials design for the next generation thermal barrier coatings", Annu. Rev. Mater. Res. 2003, 33, pp.383-417.

[2] Stott, F. H. and Wood, G. C., "Growth and Adhesion of Oxide Scales on Al_2O_3 –forming Alloys and Coatings", Mater. Sci. Eng., 87 (1987), pp.267-274.

[3] P.G. Klemens, "Phonon Scattering by Oxygen Vacancies in Ceramics", Physica B, 263-264 (1999), pp.102 – 104.

[4] Jones, R. L., "Thermal Barrier Coatings", Metallurgical and Ceramic Protective Coatings, Edited by Kurt H. Stern, Published in 1996 by Chapman & Hall, London. ISBN 0 412 54440 7.

[5] Bose, S., DeMasi-Marcin, J., "Thermal Barrier Coating Experience in the Gas Turbine Engine at Pratt & Whitney", in NASA CP3312, 1995, pp.63-78.

[6] Carlas G. Levi, "Emerging materials and processes for thermal barrier systems", Current Opinion in Solid State and Materials Science 8 (2004) pp.77-91.

[7] Sakuma, T., "Microstructural aspect on the cubic-tetragonal transformation in zirconia", Key Engineering Materials, Vol. 153-154 (1998), 75-96.

[8] Brandon, J. R. and Taylor, R., "Phase Stability of Zironia-Based Thermal Barrier Coatings Part I. Zirconia-Yttria Alloys", Surface and Coatings Technology, 46 (1991), pp.75-90.

[9] Nicholls, J. R., Lawson, K. J., "Methods to reduce the Thermal Conductivity of EB-PVD TBCs", Surface and Coating Technology, 151-152 (2002), pp.383-391.

[10] Zhu, D., Chen, Y. L., Miller, R. A., "Defect Clustering and Nano-Phase Structure Characterization of Multi-Component Rare Earth Oxide Doped Zirconia -Yttria Thermal Barrier Coatings", American Ceramic Society, V23, No. 4 (2002), pp.457-468.

[11] B. Leclercq, R. Mevrel, "Thermal conductivity of zirconia-based ceramics for thermal barrier coatings", in Proc. CIMTEC 2002, Firenze, Italy, 2002.

[12] U. Schulz, et al., "Some recent trends in research and technology of advanced thermal barrier coatings", Aerospace Science and Technology 7 (2003) 73-80.

[13] Beele, W., Marijnissen, G. and Lieshout, A. V., "The Evolution of Thermal Barrier Coatings – Status and Upcoming Solutions for Today's Key Issues", Surface and Coatings Technology 120-121 (1999), pp61-67.

[14] Hass, D. D., Slifka A. J. and Wadley, H. N. G., "Low Thermal Conductivity Vapor Deposited Zirconia Microstructures", Acta mater. 49 (2001), pp.973-983.

[15] Gu, S., Lu, T. J., Hass, D. D. and Wadley, H. N. G., "Thermal Conductivity of Zirconia Coatings with Zig-zag Pore Microstructures", Acta mater. 49 (2001), pp.2539-2547.

[16] Wolfe, D. E., Singh, J., Miller, R. A., Eldridge, J. I., and Zhu, D., "Tailored Microstructure of EB-PVD 8YSZ Thermal Barrier Coatings with Low Thermal Conductivity and High Thermal Reflectivity for Turbine Applications", Surface and Coatings Technology, In press, available 1 Jul. 2004.

[17] Luigi, V. and Clark, D. R., "High temperature aging of YSZ coatings and subsequent transformation at low temperature", Surface & Coatings Technology, 200, (2005), pp.1287-1291.

[18] U. Schulz, "Phase Transformation in EB-PVD Yttria Partially Stabilized Zirconia Thermal Barrier Coatings during Annealing", J. Am. Ceram. Soc. 83 [4] 904-10 (2000).

[19] K. Fritscher, F. Szucs, U. Schulz, B. Saruhan, M. Peters, and W. A. Kaysser, "Impact of Thermal Exposure of EB-PVDs on Young's Modulus and Sintering", Ceramic Engineering and Science Proceedings, Vol. 23, no. 4, pp.341-352, 2002.

[20] Zhao, X., Wang, X., and Xiao, P., "Sintering and failure behavior of EB-PVD thermal barrier coating after isothermal treatment", Surface & Coatings Technology, in press, (2005)

[21] Rabiei, A. and Evans, A. G.., "Failure mechanisms associated with the thermally growrn oxide in plasma-sprayed thermal barrier coatings", Acta. Mater., 48 (2000), pp. 3963-3976.

[22] Alperine, S., Derrien, M., "Thermal Barrier Coatings: the Thermal Conductivity Challenge", NATO Workshop on Thermal Barrier Coatings, Aalborg, Denmark, AGARD-R-823 (1998), pp.1

[23] Zhu, Dongming, Bansal, N. P., Miller, R. A., "Thermal conductivity and stability of HfO_2-Y_2O_3 and $La_2Zr_2O_7$ evaluated for 1650^0C thermal/environmental barrier coating applications", Ceramic Transactions, V153, 2004, P331-343.

[24] Youngblood, G. E., Rice, R. W., Ingel, R. P., "Thermal Diffusivity of Partially and Fully stabilized (Yttria) Zirconia Single Crystals", J. Am. Ceram. Soc., 71(4), 1988, p255-260.

[25] Eldridge, J. I., Spuckler, C. M., and Street, K.W., "Infrared Radiative Properties of Yttria-Stabilized Zirconia Thermal Barrier Coatings", 26th Annual Conference of Composites, Advanced Ceramics, Materials and Structures: B, Cocoa Beach, FL, Jan. 13-18, 2002, Westerville, OH, American Ceramic Society (2002), pp.417-430.

[26] R. Siegel, C. M. Spuckler, "Analysis of Thermal Radiation Effects on Temperatures in Turbine Engine Thermal Barrier Coatings", Materials Science and Engineering, A245 (1998), pp.150-159.

[27] Minervini, L., Grimes, R. W., "Disorder in Pyrochlore Oxides", J. Am. Ceram. Soc., 83 (8) (2000), pp. 1873 –1878.

[28] Stanek, C. R., Minervini, L. and Grimes, R. W., "Nonstoichiometry in $A_2B_2O_7$ Pyrochlores", J. Am. Ceram. Soc., 85 [11], pp.2792-98, 2002.

[29] Lehmann H., Pitzer D., Pracht G., Vassen R., and Stőver D., "Thermal conductivity and thermal expansion coefficients of the lanthanum rare-earth-element zirconate system", J. Am. Ceram. Soc., 86[8], 2003, 1338-1344.

[30] Berman, R., "Thermal Conduction in Solids", Clarendon Press, Oxford, UK, 1976.

[31] Klemens, P.G., Thermal Conductivity, Vol. 1, edited by R. P. Tyne (Academic Press, London, UK, (1969).

[32] Wu J., Wen X., Padture N. P., Klemens P. G., Gell M., Garcia E., Miranzo P., Osendi M. I., "Low thermal conductivity rare earth zirconates for potential thermal barrier coating applications", J. Am. Ceram. Soc., 85[12], 2002, 3031-3035.

[33] Maloney, M. J., Thermal Barrier Coating Systems and Materials, US Patent 6,231,991 B1, (2001).

[34] Catcher G. L. and Rearick T. M., "O-anion transport measured in several $R_2M_2O_7$ pyrochlores using perturbed – angular correction spectroscopy", Phys. Rev. B, B52, 1995, 9890-9899.

[35] Van Dijk M. P., Vries K. J. D. and Burggroaf A. J., "Oxygen ion and mixed conductivity in compounds with the fluorite and pyrochlore structure", Solid State Ionics, 9-10, 1983, 913-20.

[36] Mori, M., Abe, T., Itoh, H., Yamamoto, O., Shen, G. Q., Takeda, Y. and Imanishi, N., Reaction Mechanism Between Lanthanum Manganite and Yttria Doped Cubic Zirconia, Solid State Ionics Vol. 123, 1999, pp.113-119.

[37] Vassen R., Cao X., Tieta F., Basu D., and Stőver D., "Zirconates as new materials for thermal barrier coatings", J. Am. Ceram. Soc., 83[8], 2000, 2023-2028.

[38] Cao XQ, Vassen R., Stőver D., "Ceramic materials for thermal barrier coatings", J. Eur. Ceram. Soc. 2004; 24.

[39] Carlas G. Levi, "Emerging materials and processes for thermal barrier systems", Current Opinion in Solid State and Materials Science 8 (2004) 77-91.

[40] R. Siegel, J. R. Howell, Thermal Radiation Heat Transfer, Taylor & Francis; 4th edition (December 15, 2001).

[41] H. A. Macleod, Thin-film Optical Filters, 2nd ed., Published by Adam Hiller Ltd. (1986) 158-186.

[42] Wang D, Huang X, Patnaik PC. Design and Modeling of Multiple Layered TBC System with High Reflectance, Journal of Material and Science (2005) In Press.

[43] Stőver, D., Pracht, G., Lehmann, H., Dietrich, M., Dőring, J-E. and Vaβen, R., New Material Concepts for the Next Generation of Plasma-Sprayed Thermal Barrier Coatings, Journal of Thermal Spray Technology, Vol. 13 (1), pp.76-83, 2004

[44] Zhu, Dongming, Chen, Yuan L., Miller, R. A., Defect Clustering and Nano-Phase Structure Characterization of Multi-Component Rare Earth Oxide Doped Zirconia -Yttria Thermal Barrier Coatings, American Ceramic Society, V23, No. 4 (2002), p.457-468.

[45] J. R. Nicholls, K. J. Lawson, Low Thermal Conductivity EB-PVD Thermal Barrier Coatings, Material Science Forum, 369 – 372 (2001), p. 595-606.

[46] W. P. Allen, Reflective Coatings to Reduce Radiation Heat Transfer, US patent US 0008170 A1, (2003).

[47] P. G. Klemens, Theory of Thermal Conductivity of Nanophase Material, Chemistry and Physics of Nanostructures and Related Non-Equilibrium Materials, ed. E. Ma and B. Fultz, The Minerals, Metals & Materials Society (1997).

[48] J. Singh, D.E. Wolfe, Review: Nano and Macro-Structured Component Fabrication by Electron Beam-Physical Vapor Deposition (EB-PVD), J. Mater. Sci., 40 (2005) 1-26.